

## CHAPTER II

### THEORETICAL BACKGROUND AND LITERATURE REVIEW

#### 2.1 Silk sericin

##### 2.1.1 Overview of silk sericin

Silk is a natural protein fiber has been widely use in textile industry for a long period of time because of its mechanical properties and luster. Most commercial silk produced from mulberry silk worm, *Bombyx mori* belongs to Bombycidae family. The formation of silk cocoon composed of two major proteins named fibroin and sericin. Fibroin is the core protein constituted over 70% of cocoon and surrounding by sericin the “glue like” protein constituted 20-30% of cocoon. Sericin must be removed from fibroin during raw silk manufacturing by degumming process and usually discarded in silk waste water lead to the water pollution because of high value of COD and BOD. (Kundu *et al.*,2008)

Silk sericin is hydrophilic glycoprotein contains 18 amino acids and most of which have strongly polar side groups. The hydrophilicity of silk sericin comes from high amino acid serine content. Its molecular weight ranges widely from 10 to over 300 kDa. The structure of silk sericin mainly occurs in amorphous random coil and less  $\beta$ -sheet structure with 63% and 35%, respectively (Kunda *et al.*, 2008, Zhang, 2002). The sol-gel phenomena of silk sericin solution occurs since the random coil structure is soluble in water and when the temperature is lower the random coil structure turn to  $\beta$ -sheet structure resulting in the gel formation (Padamwar *et al.*, 2004).

Vaithanomsat *et al.*, 2008 studied on the separation of silk sericin from silk waste water derived from silk manufacturer in Thailand. They determined the amino acid composition in silk sericin which is extracted from waste water compared with silk sericin extracted by hot water and silk sericin raw material as shown in Table 2.1.

**Table 2.1** Amino acid composition in degumming solution compared with reference sericin (Vaithanomsat *et al.*, 2008)

Amino acid	Percent of gram amino acid in 100 g protein		
	Sericin raw material	Degumming solution <sup>a</sup>	Hot water-soluble sericin <sup>b</sup>
Aspartic acid	15.74	14.95	17.97
Serine	31.99	38.81	28.00
Glutamic acid	6.28	3.93	6.25
Glycine	14.20	14.45	16.29
Histidine	1.49	Not detected	1.32
Arginine	4.29	3.27	3.52
Threonine	7.73	7.79	7.78
Alanine	4.85	5.13	5.20
Proline	0.71	0.47	Not detected
Cryptine	0.20	Not detected	0.69
Tyrosine	3.01	2.44	2.87
Valine	3.30	3.33	3.77
Methionine	Not detect	Not detected	Not detected
Lysine	4.17	3.12	3.72
Isoleucine	0.72	0.77	0.79
Leucine	0.96	1.18	1.21
Phenylalanine	0.37	0.34	0.64

<sup>a</sup> From laboratory analysis

<sup>b</sup> From reference

### 2.1.2 Degumming process

In silk manufacturing, silk sericin is separated from fibroin by degumming process which based on solubility of silk sericin. There are several methods to remove sericin such as using heat, acid solution, alkaline solution and enzymes. Degumming by heat or heat under pressure has an advantage because an obtained silk sericin is less impurity. Using acid to remove sericin is more hazardous than using alkaline. Almost silk industrial uses the extraction with soaps and detergents since it is a simple process compared with other processes. (Aramwit *et al.*, 2012) Padamwar *et al.* (2004) review many methods to degumming silk sericin. They reported that most of silk sericin was removed by autoclaved under pressure of

600-700 mmHg (0.8-0.9 atm) for one and a half hour. The satisfying yield was obtained from autoclaving at 105°C for 30 min with good gelling property and yield.

Several methods have been carried out to recovery silk sericin from degumming waste water such as freeze drying, spray drying, membrane filtration, enzymatic hydrolysis and precipitation by ethanol (Aramwit *et al.*, 2012)

Vaithanomsat *et al.* (2008) studied on the methods to recover silk sericin compared between tray-drying and freeze-drying. They suggested that both drying methods gave the similar yield of recovered silk sericin powder with the similar composition excepted water solubility. The freeze-dried sericin was completely soluble in water but tray-dried sericin was dissolved only 96.28% in water. Hence, the heating process of tray-drying denatured protein in silk sericin resulting in the formation of thin film on the top of the silk sericin solution's surface during tested for water solubility. Therefore, they suggested to use freeze-drying in order to dry silk sericin in the other experimental.

### 2.1.3 Application of silk sericin

The application of silk sericin widely ranges from cosmetics to biomedical products. Silk sericin is biocompatible and biodegradable materials due to its protein nature which sensitive to proteolytic enzymes in the human body and digestible (Padamwar *et al.*, 2004). Because of high polar amino acid which consists of polar side chain such as hydroxyl, carboxyl and amino groups makes silk sericin easy to cross-linking, copolymerization and blending with other polymer to improve the biodegradable properties (Dash *et al.*, 2009).

Low molecular weight silk sericin is used in cosmetics for skin, hair and nails. Silk sericin enhances skin elasticity and exhibited anti-winkle and anti-aging effect. In the gel form, it has the moisturizing property thus it always used in lotion and cream. Moreover, sericin is used in nail cosmetics to prevent nail brittleness and shampoo for cleaning hair. In medical and pharmaceutical applications, silk sericin has been used as antioxidants, anticancer drug, wound dressing, drug delivery and film or hydrogel for tissue engineering etc. (Kundu *et al.*, 2008).

Sarovart *et al.* (2003) studied on the use of silk sericin in order to enhance the antioxidant, antifungal, and antimicrobial properties of indoor air filters by coating the filters with silk sericin extracted from three different species of Thai silk cocoon: Nang Noi, Dok bua and Jul. From FTIR spectra as shown in Figure 2.1, silk sericin Dok Bua and Nang Noi had higher absorbance than Jul indicated that silk sericin Dok Bua and Nang Noi have 18 amino acids and silk sericin Jul has only 14 amino acids. Furthermore, they found that as increasing in the concentration of silk sericin, the antioxidant, antifungal and antibacterial efficiency in *Micrococcus* type was increased and the efficiency was dissimilar with different species.

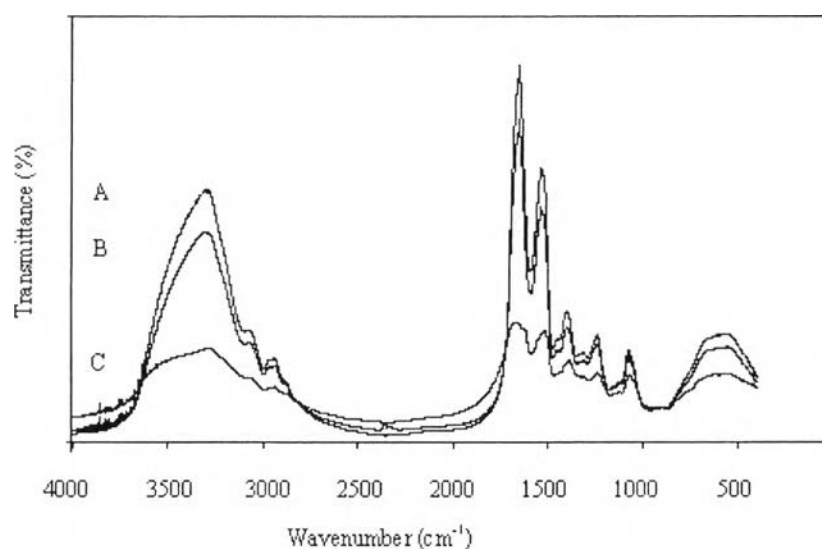


**Figure 2.1** FTIR spectra of (A) sericin Dok-Bua, (B) sericin Nang-Noi, (C) sericin Jul (Sarovat *et al.*, 2003).

There are several studies on the use of silk sericin in medical and cell culture applications. Tsubouchi *et al.* (2005) studied on the efficiency of silk sericin to enhance the attachment of human skin fibroblasts. They extracted silk sericin from the silk cocoon and coated on Petri dishes in order to culture the human skin fibroblast cells. The test was compared with collagen, which is generally used as a cell culture substratum. After cultured the cells on Petri dishes coated with silk sericin for 72 hr, the cell proliferation rate was similar to the non-coated control and the collagen-coated control. The cell growth of silk sericin-coated showed well

extended fibrous shape similar to collagen-coated indicated that silk sericin can be a good candidate for use as substratum for cultivation of human skin fibroblast cell.

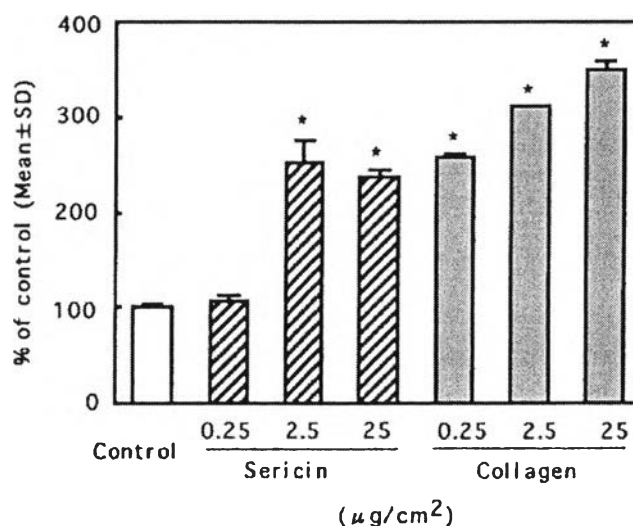


**Figure 2.2** Effect of silk sericin and collagen on the attachment of Human Skin Fibroblasts (Tsubouchi *et al.* 2005).

Takeuchi *et al.* (2005) studied the heterogeneous nucleation of hydroxyapatite on silk sericin film. Hydroxyapatite is the form of calcium phosphate which is the important component in bone and teeth. In this work, they used simulated body fluid (SBF) to reproduce hydroxyapatite. After degumming, silk sericin films containing  $6 \text{ mg ml}^{-1}$  were fabricated by drying solution under ambient condition and by casting solution in Petri dish. From GPC results, the most frequent distribution in Mw appeared at 159 and 43 kDa. The structure of silk sericin was mostly random coil indicated from CD spectrum but after stored silk sericin at  $4^\circ\text{C}$  for 2 weeks, the content of  $\beta$ -sheet was increased. They suggested that the hydroxyapatite deposition was observed in silk sericin film which using the extracted temperature was  $105^\circ\text{C}$  and stored for 2 weeks as shown in Figure 2.3 because it had the highest content of  $\beta$ -sheet structure.

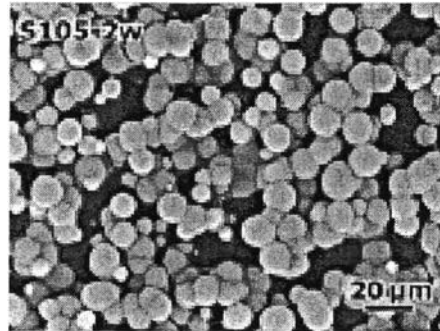


**Figure 2.3** SEM images of the surfaces of sericin films prepared from various solutions after soaking in the 1.5 SBF for 7 days (Takeuchi *et al.*, 2005).

Not only the  $\beta$ -sheet structure content but the molecular weight of silk sericin also influence on the nucleation of hydroxyapatite. The inducement of hydroxyapatite also depend on the carboxyl group content and their arrangement, thus a higher molecular weight lead to a specific relationship between each  $\beta$ -sheet in the silk sericin molecular structure. Due to the carboxyl groups were effective in the nucleation of hydroxyapatite from a solution hence silk sericin had the efficiency for this application.

Silk sericin has been studied in the form of porous material for biodegradable purpose and medical application. Porous structure of silk sericin via freeze-drying process was investigated by Tao *et al.* (2005). They studied on the effect of temperature and concentration of silk sericin solution on the structure and properties of porous material. Silk sericin was extracted from silk cocoon to obtain silk sericin solution with the concentration of 1.1% by weight and diluted to 0.7% and 0.3% by deionized water. The porous silk sericin were prepared via freeze-drying process by using Poly(ethylene glycol) diglycidyl ether as cross-linked agent. The morphology of porous sericin is shown in Figure 2.4. They found that the decreasing of freezing temperature and increasing of silk sericin concentration resulting in the decreasing of pore size and porosity but pore density was increased. The XRD curves indicated the mainly structure of porous silk sericin was amorphous

with a few content of  $\beta$ -sheet. The cross-linked sample the  $\beta$ -sheet structure was increased.

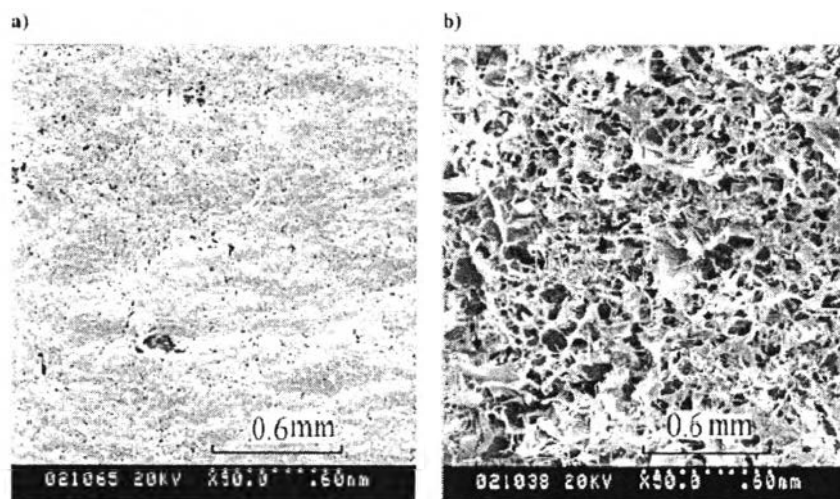


**Figure 2.4** Scanning electron microscope (SEM) photographs of porous sericin material's surface. (a) Top-surface; (b) under-surface (Tao *et al.*, 2005).

Due to silk sericin forms fragile materials that may not be suitable for some medical applications hence blended with other materials can be solved this problem. Silk sericin blended with hydrophilic polymer such as gelatin, collagen and PVA was studied by Mandel *et al.* (2009) and Aramwit *et al.* (2010). They found that after blending, silk sericin can form scaffold and can be a good candidate for tissue engineering due to its biocompatible and non-cytotoxicity. Moreover, silk sericin enhanced the attachment and viability of cell.

Mandel *et al.* (2009) studied on the sericin/gelatin 3-D scaffold and 2-D film for tissue engineering application. They used sericin which extracted from *A. mylitta*, a non-mulberry silkworm, blended with gelatin and using glutaraldehyde as cross-linking agent with HCl as group-activating agent. The films were casted on teflon-coated plate and the scaffolds were prepared by freeze-drying process. They found that increasing of gelatin concentration enhanced mechanical strength of scaffold and the lower of sericin content gave higher the compressive strength. In addition, the increasing of sericin content resulting in the increasing of porosity and

enhanced the cell migration, cell attachment and the passage of nutrients to growing cells. They reported that sericin/gelatin blends were cytocompatibility for fibroblast cells. However, at the higher content of sericin about 5 and 7.5%, cell growth and mitochondrial activity were decreased due to the high leaching of sericin molecules. The highest activity of cells was observed at 2wt% of sericin blended with 5wt% gelatin which similar to the control when grown for 4 days.

Aramwit *et al.* (2010) studied on the silk sericin-PVA three-dimensional scaffold by using freeze-drying process. Silk sericin solution and PVA solution with and without glycerin were mixed together to make a wet composition of sericin and PVA ranging from 1-5 w/v% and glycerin 1 w/v%. (Glycerin was used as plasticizer to reduce phase separation between silk and PVA blend). Genipin solution (cross-linked agent) with varying concentration between 0.01-0.1 w/v% was added in to the mixed solution followed by freeze-drying in lyophilizer. They reported that the most suitable composition of silk sericin and PVA to make homogenous and stable matrix was sericin 3 w/v%, PVA 2 w/v% and glycerin 1 w/v% of wet weight. From their results, uncross-linked silk sericin/PVA scaffold was rigid, less flexible, less ability to absorb moisture and higher release of silk sericin when compared with sericin/PVA/glycerin with genipin cross-linked. Therefore, silk sericin/PVA/glycerin especially with 0.1% genipin seem to be a good candidate for biomaterials for tissue engineering because of its good moisture absorption, high swelling degree and good mechanical strength.

Takeuchi *et al.* (2005) studied on the porous structure of alpha-tricalcium phosphate coated with silk sericin used for bone regeneration in rabbit tibiae. The porous structure of  $\alpha$ -TCP was coated with silk sericin by soaking in the silk sericin solution in vacuum for 1 h. The samples were implanted into the bone defects made in rabbit tibiae and back to observe the bone regeneration for 4 weeks. They found that  $\alpha$ -TCP coated with silk sericin gave higher bone regeneration and bone density. The pQCT images of rabbit tibiae which implanted with  $\alpha$ -TCP and  $\alpha$ -TCP/sericin for 4 weeks as shown in Figure 2.5 and the density histograms of rabbit tibiae where  $\alpha$ -TCP and  $\alpha$ -TCP/sericin were implanted for 4 weeks as shown in Figure 2.6. Silk sericin coated  $\alpha$ -TCP showed slower degradation than neat  $\alpha$ -TCP thus it may be useful for production of biodegradable materials for bone repair.



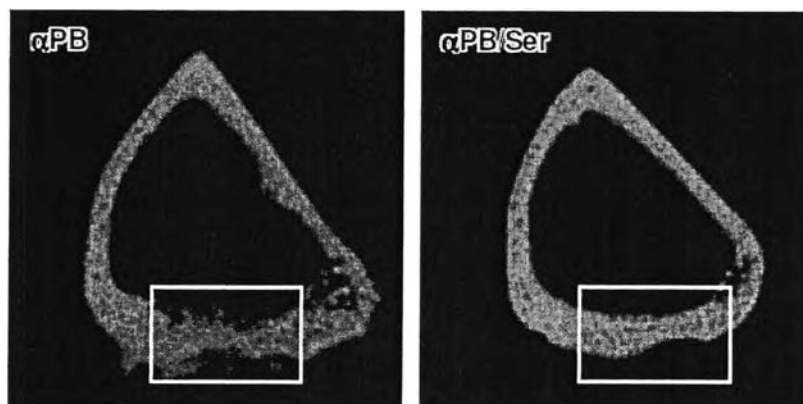


**Figure 2.5** Peripheral quantitative computed tomography (pQCT) images of rabbit tibiae. The squares on the images indicate the sites where  $\alpha$ -PB and  $\alpha$ -PB/Ser were implanted for 4 weeks (Takeuchi *et al.*, 2005).

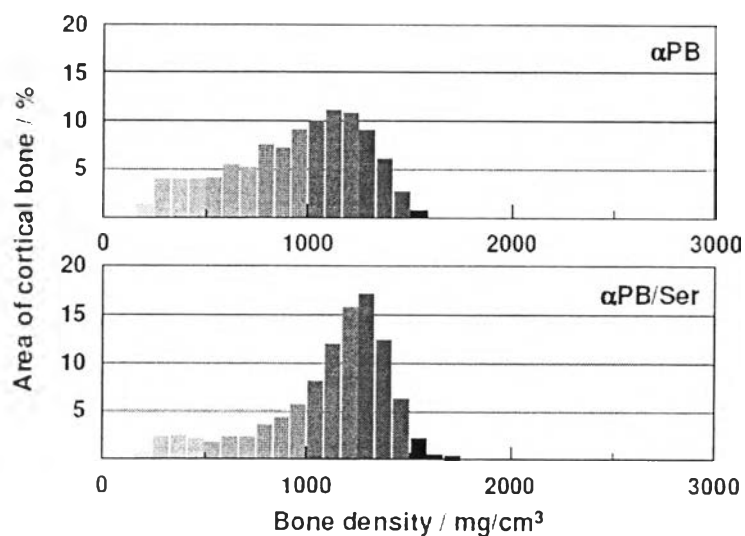


**Figure 2.6** Density histograms of rabbit tibiae where  $\alpha$ -PB and  $\alpha$ -PB/Ser were implanted for 4 weeks (Takeuchi *et al.*, 2005).

## 2.2 Clay mineral – Sodium bentonite

### 2.2.1 Overview of bentonite clay

The smectite clays are valuable minerals widely used in many applications. Smectites is the family name which includes sodium and calcium montmorillonites. The rock that dominantly composed of smectite minerals is generally called bentonite. (Murray, 1991)

Bentonite formed from the alternative of volcanoclastic or pyroclastic rock and it is composed of montmorillonite (Karakaya *et al.*, 2011). Smectites are the three-layer clay mineral which composed of two silica tetrahedral sheets joined to a central octahedral sheet of either aluminum or magnesium hydroxide to form as a 2:1 layer or phyllosilicates. The layer thickness is around 1 nm and the lateral dimensions of these layers may vary from 30 nm to several microns or larger depending on the particular layered silicate. Stacking of the layers leads to a regular van der Waals gap between the layers called the interlayer or gallery. There are some substitutions of  $\text{Fe}^{2+}$  and  $\text{Mg}^{2+}$  for  $\text{Al}^{3+}$  in the octahedral sheet and also some substitutions of  $\text{Al}^{3+}$  for  $\text{Li}^{1+}$  in the tetrahedral sheets. The substitution creates a negative charge imbalance which is about -0.66/unit cell. The net positive charge deficiency is balanced by exchangeable cation adsorbed between the unit layers and around the edges. If the exchangeable cation is sodium, the specific mineral is sodium montmorillonite. (Murray, 1991, Ray *et al.*, 2003 ) Figure 2.7 shows the structure of 2:1 phyllosilicates and Table 2.2 introduces the chemical formula and characteristic parameter of 2:1 phyllosilicates.

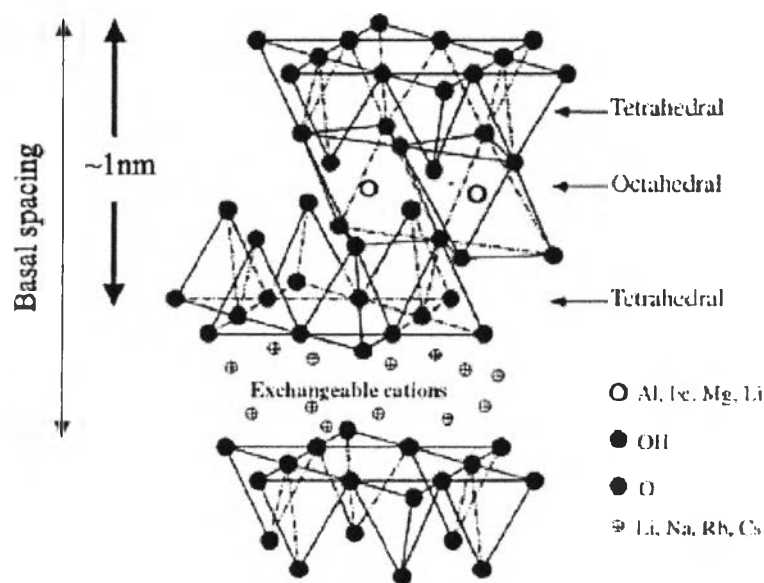


**Figure 2.7** Diagrammatic sketch of the structure of smectites (Ray et al., 2003).

**Table 2.2** Chemical formula and characteristic parameter of commonly used 2:1 phyllosilicates (Ray et al., 2003)

2:1 phyllosilicates	Chemical formula	CEC (mequiv/100g)	Partical length (nm)
Montmorillonite	$M_x(Al_{4-x}Mg_x)Si_8O_{20}(OH)_4$	110	100-150
Hectorite	$M_x(Mg_{6-x}Li_x)Si_8O_{20}(OH)_4$	120	200-300
Saponite	$M_xMg_6(Si_{8-x}Al_x)Si_8O_{20}(OH)_4$	86.6	50-60

where M is monovalent cation and x is degree of isomorphous substitution (between 0.5 and 1.3).

Sodium montmorillonite which is the major component of sodium bentonite generally have one water layer in the interlayer position and the basal spacing is 12.2 Å. It is high-swelling clay when placed in water; it will expand up to 10 or more times than dry volume. The cations and water layers can be replaced by polar organic molecules such as ethylene glycol, quaternary amine, polyalcohol and

others. This is an important property which can be translated into useful products. (Murray, 1991)

### 2.2.2 Polymer/clay nanocomposite

Layered silicate clay has a very high aspect ratio. A few weight percent of clay are suitably for dispersed clay into the polymer matrix and creates high surface area for polymer/clay interaction. The structure of polymer/clay nanocomposites can be classified in to three different types:

1. **Intercalated structure** which the insertion of polymer chains into the clay structure occurs only in a crystallographically regular fashion. Intercalated nanocomposites are normally interlayer by a few molecular layers of polymer.
2. **Flocculated structure** which is the same as intercalated nanocomposites but sometimes clay are flocculated because of hydroxylated edge–edge interaction of the silicate layers.
3. **Exfoliated structure** which the individual clay layers are separated in a continuous polymer matrix by an average distances depends on clay loading.

Clay usually is in the intercalated form more than exfoliated form. However, the exfoliated structure is more required because it give the superior reinforcing efficiency. (Ray *et al.*, 2003, Pojanavaraphan *et al.*,2008)

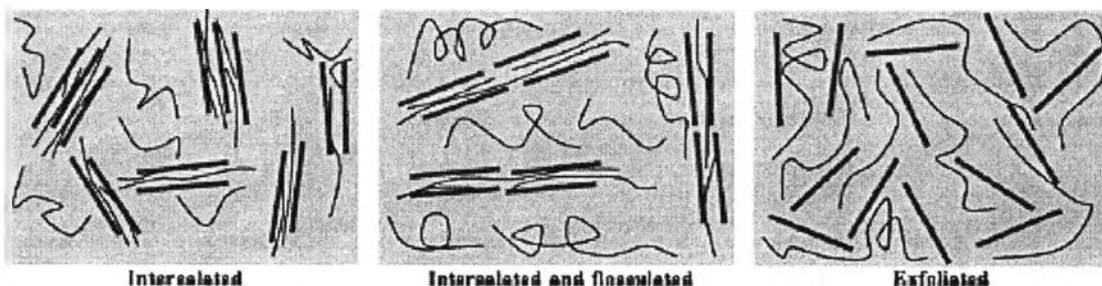


**Figure 2.8** Schematically illustration of three different types of achievable polymer/clay nanocomposites (Ray *et al.*, 2003).

Meieszawska *et al.* (2011) studied silk fibroin/clay film using as composite for bone tissue engineering which silk fibroin acted as a supportive

biomaterial and montmorillonite clay (MMT) acted as a source of osteo-inductive silica species. The silk/clay film studied with human mesenchymal stem cells (hMSC). After degumming, silk fibroin was dissolved in 9.3 M LiBr and dialyzed against 18.2 MΩ deionized water, the final concentration of silk solution was 8 wt%. Then silk fibroin solution mixed with MMT with the concentration of MMT was 0.32, 0.65 and 1.4 wt%. They found that silk/MMT film showed good adhesive and proliferation without cell detachment from the film. The high viability of hMSC on the silk/clay surface observed at 0.32% MMT and the viability decreased with the increasing of clay particles.

Haroun *et al.* (2009) invented the 3-D gelatin-montmorillonite/cellulose scaffold for tissue engineering application. MMT suspension was mixed with gelatin and cellulose solution using glutaraldehyde (GT) solution or N, N-methylene-bisacrylamide (MBA) as crosslinking agents. The mixtures were frozen at -80°C for 12 hr and lyophilized in freeze-dryer for 48 hr. They found that increasing of MMT resulted in the decreasing of water absorption. When the content of clay increased, the degradation was decreased. Degradation rate was depended on the content of crosslink agent. From XRD patterns, the increasing of interlayer spacing indicated the intercalation of MMT due to the insertion of gelatin molecules into the sheets of MMT. The pores size of G-MMT-Cel with 6% MMT was around 300 μm. As the content of MMT increased, the pore shape was irregular with lower interconnection degree. In cell cultured study which studied on the human mesenchymal stem cells (Saos-2 cells) showed that MMT was the important factors effect on the cell activities. After seeding cell more than 16 days, the scaffold with the presence of MMT showed high efficient for cell adhesion, penetration and cluster formation especially the scaffold contained 6%Gel/6%Cel/12%MMT/5%GT (scaffold 6) and 6%Gel/6%MMT/0.5%GT (scaffold 8). Furthermore, the scaffold 6 and scaffold 8 showed the significant induction in cell proliferation, cell nuclear antigen proliferation and alkaline phosphatase production.

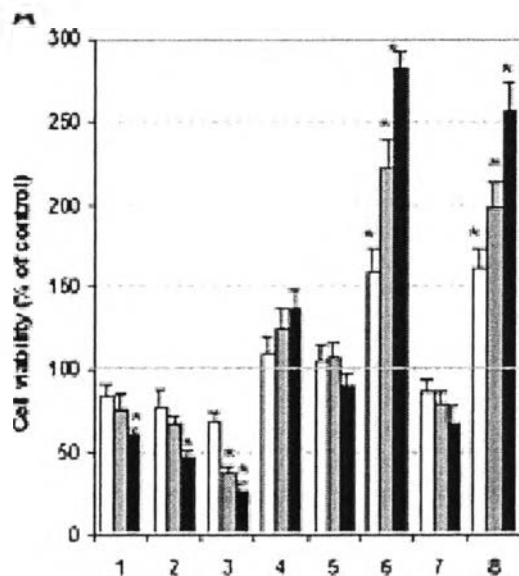


**Figure 2.9** The effect of the incubation with different biocomposites (10 mg/ml) for variable intervals 4 days (white bars), 8 days (graybars), and 16 days (black bars) on the proliferation rate of Saos-2cells (Haroun *et al.*, 2009).

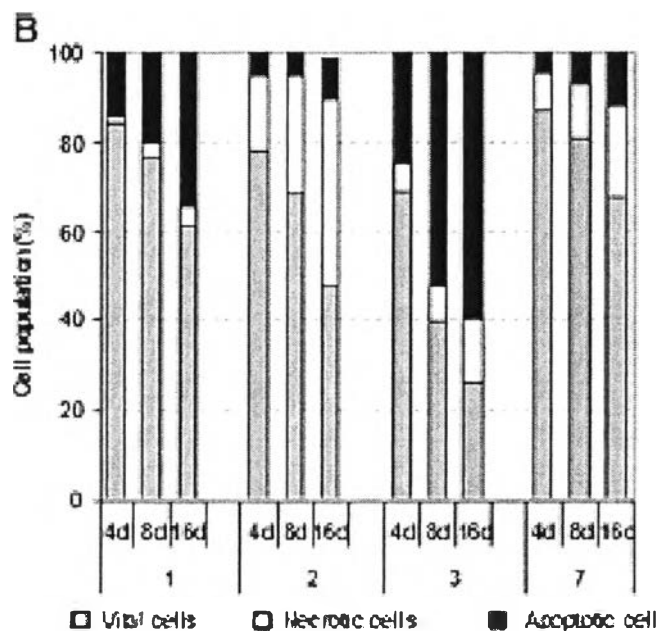


**Figure 2.10** The type of death in Saos-2 cells after being seeded with 10 mg/ml of cytotoxic biocomposites 1, 2, 3, and 7 for 16 days (Haroun *et al.*, 2009).

The scaffold contained high content of GT gave high apoptosis and necrosis (determined the extent of death cells) because of the released residual

uncross-linked GT. They suggested that incorporation of MMT fulfilled the properties of biocomposite to achieve the requirements for 3-D scaffold for tissue engineering hence MMT improved cytocompatibility between the osteoblast and biocomposite.

### 2.2.3 Clay aerogel

Aerogel was first described in 1932 by Kistler. Aerogel is used to express the inorganic gels which the liquid was replaced with gas without collapsing the solid network. The bulk density of aerogel is in the range of 0.01-0.1 g/cm<sup>3</sup>. Aerogel has a very high relative and specific pore volume depend on the nature of solid materials. Normally, the relative pore volume of aerogel is about 90% in the study of silica aerogels but may be lower in other type of aerogels. (Aegerter *et al.*, 2011, Bandi *et al.*,2005)

Layered clay can be rearrangement to house of cards like aerogels structure by freeze-drying process. Mackenzie and Call was found the preparation of montmorillonite clay aerogels by freeze-drying clay hydrogels resulted in fibrous montmorillonite structures. The clay aerogel has rigidity, but poor thermal stability at 110°C. In 1967, Van Olphen described that the house of card structure of clay aerogel was occurred because of the opposite edge and face electrostatic charge. The faces have negative charges on siloxane surface and the edges have positive charges of alumina sheet resulting in the charge attraction. When clays are frozen, the ice crystals are growing and push the particles aside to encourage the parallel alignment. The ice crystals are sublimed under vacuum, the porous is fulfilled by the air instead of water resulting in the high porosity and low density materials (Pojanavaraphanet *et al.*,2008, Bandi, 2006).

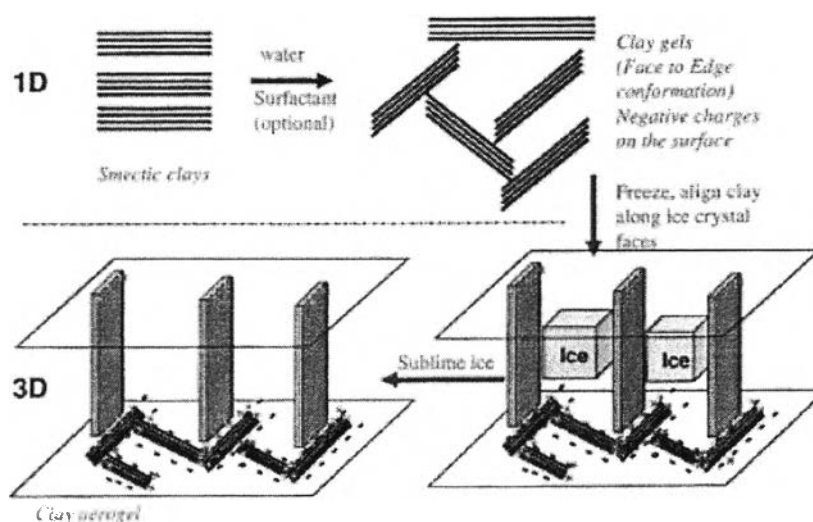


**Figure 2.11** Synthesis of clay aerogels (Somlai *et al.*2006).

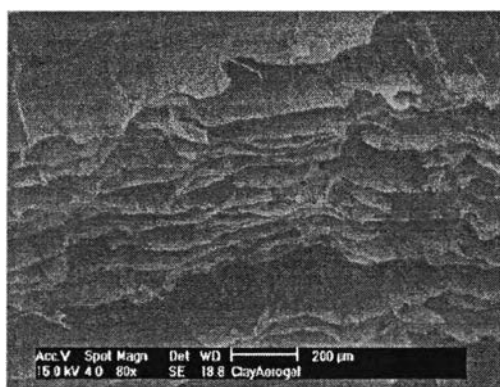


**Figure 2.12** SEM image of freeze dried clay to form Clay Aerogel ("house of card" sheet-like structure) super gallery spacing  $\sim 200\mu\text{m}$ . (Bandi, 2006).

Neat clay aerogels are relatively fragile and exhibit low mechanical properties thus they are easy to break and damage under low stress level. To overcome this problem, the combination of polymeric materials or fibers into the clay aerogels are required. The incorporation polymer into clay aerogels can be improved mechanical properties, produced the form-like structure and also expanded the range of applications. Many polymer/clay aerogel composites were investigated



such as natural rubber/clay aerogel composite, PNIPAM/clay aerogel composite, silk fibroin/clay aerogel biocomposite and casein/clay aerogel biocomposite (Pojanavaraphan *et al.*, 2008, Pojanavaraphan *et al.*, 2010, Bandi *et al.*, 2005, Finlay *et al.*, 2008)

Somlai *et al.* (2006) studied on the organically-modified clay aerogel by using sodium-exchanged, 12-aminolauric acid exchanged and octadecyltrimethyl quaternary amine salt exchanged montmorillonite. The organoclay was dispersed in water and mixed with HCl and surfactant. The mixture were frozen with  $-80^{\circ}\text{C}$  and evacuated for 36 hr in freeze-dryer. After freezing the clay suspension for 1 hr, the highly ordered ice-clay patterns were observed. After vacuum for 48 hr, a soft stacked layer and highly ordered with a sheet texture liked was produced with interlayer voids were approximately 100-200  $\mu\text{m}$ . They introduced the morphology formation of clay aerogel according to Nakazawa *et al.*'s research as shown in Figure 2.13. They reported the process parameter such as shear rate, surfactant and freezing condition were affected to the formation of aerogel structure. Moreover, the concentration of clay in water was important feature because the concentration less than or equal 0.7 wt% did not form aerogel structure and the concentration above 2.9 wt% were viscous and difficult to blend. From WAXD indicated that surfactant was intercalated in to clay gallery due to the increasing of  $d_{001}$  spacing.

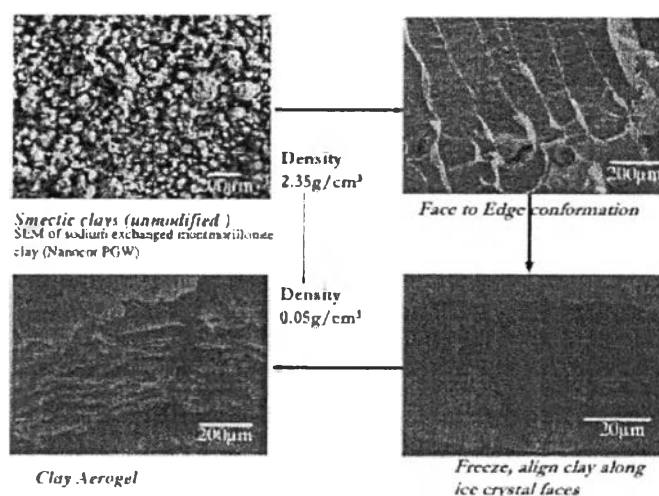
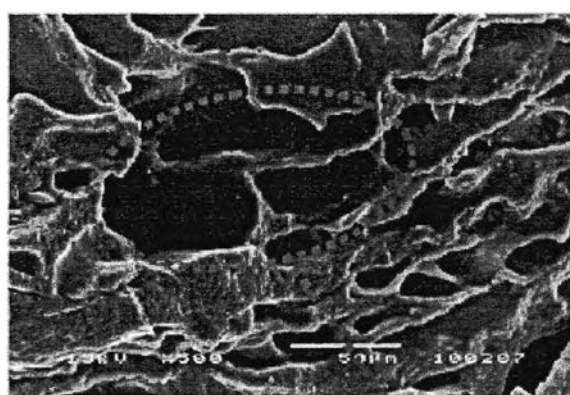


**Figure 2.13** The morphology formation of clay aerogel (Somlai *et al.*, 2005).

In 2008, Pojanavaraphan *et al.* invented the prevulcanized natural rubber latex/clay aerogel nanocomposites using pristine clay (Na-montmorillonite). The Na-MMT content was varying in 1-3 phr in order to study the effect of clay in NR matrix. The prevulcanized NR latex was mixed with the dispersion of pristine clay followed by stirring for 30 min at room temperature. Then the mixture immediately frozen in cylindrical glass shells at liquid nitrogen temperature and sublimed the ice in freeze-dryer maintained at  $-54^{\circ}\text{C}$  under vacuum for 36 h. The samples were vulcanization under two methods including thermal curing and microwave curing. They found that the neat Na-MMT aerogel was not an exfoliated structure but only appeared as clay bundles. In case of NR/MMT, the XRD patterns showed the increasing of  $d_{001}$  spacing indicated that rubber intercalated in the clay plates. In addition, nanocomposite with 3 phr MMT had no diffraction peak, which indicated the exfoliation of clay platelets. In case of nanocomposite with 1 and 2 phr MMT, showed the clay content was not enough to create the aerogel structure. On the other hand, the aerogel structure began to form in NR/3MMT. The SEM micrograph of NR/3MMT is shown in Figure 2.14.



Aerogel structure

**Figure 2.14** SEM micrograph of NR/3MMT (Pojanavaraphan *et al.*, 2008).

Furthermore, hardness of the aerogel increased with the increasing of MMT content. In this work, it had the interesting point in the thermogravimetric analysis. They found that the onset and peak of degradation temperature of aerogels were slightly decreased with increasing of MMT content due to the acceleration in the thermal degradation of NR by  $\text{Fe}^{3+}$  isomorphously substituted in the octahedral sheet of Na-MMT clay.

Afterward, Pojanavaraphan *et al.* (2010) also studied on the mechanical, rheological and swelling behavior of natural rubber/montmorillonite aerogels by freeze-drying process. The prevulcanization NR latex contained 60% NR mass was diluted to 30% NR mass and slowly mixed with Na-MMT dispersion in different contents. The mixture was frozen in cylindrical glass vials at  $-80^{\circ}\text{C}$ . The frozen samples were transfer to freeze-dryer with condenser temperature at  $-108^{\circ}\text{C}$  for 3 days. The XRD patterns indicated that the composites were intercalated because of the increasing of basal spacing. SEM micrographs showed that only in the case of composites with 5 and 7 phr Na-MMT was observed the regular layered morphology and completely covered by NR layers. To achieve the aerogels structure, they suggested that Na-MMT at least 2% MMT was required. The swelling behavior of aerogel was determined by the equilibrium solvent uptake. The result showed the equilibrium solvent uptake increased with increasing of Na-MMT content and decreasing of cross-linking density. From the compression test and DMA indicted that the mechanical properties increased with the increasing of Na-MMT content. The composites were stiffer due to the reinforcing effect of Na-MMT. The present of voids was observed especially in the composites contained 7 phr Na-MMT.

**Table 2.3** The initial modulus and reinforcing efficiency of nanocomposites (Pojanavaraphan *et al.*, 2010)

<b>Samples</b>	<b>Initial modulus (kPa)</b>	<b>Reinforcing efficiency (%)</b>
PNR	17.3 ± 6.3	-
PNR/M1	19.3 ± 7.1	14.6
PNR/M3	23.0 ± 4.5	29.1
PNR/M5	22.5 ± 4.0	22.7
PNR/M7	35.4 ± 11.8	80.7

Lui *et al.*, (2011) prepared the chitosan/xanthan gum/montmorillonite macro porous by using freeze-drying method. The mixture of chitosan and xanthan gum was mixed with suspension unmodified Na-MMT clay. They investigated the effect of the freezing rate and freezing process; immersion freezing and contact freezing on the formation of the macro porous foams. They found that the addition of Na-MMT exhibited the greater rigidity and increased the mechanical strength of freeze-dried foams when compared with the freeze-dried foam from only chitosan/xanthan gum. The hardness was increased when incorporate Na-MMT into the nanocomposite and the highest hardness value was observed in sample that prepared at slow freezing rate with the presence of Na-MMT as shown in Figure 2.15.

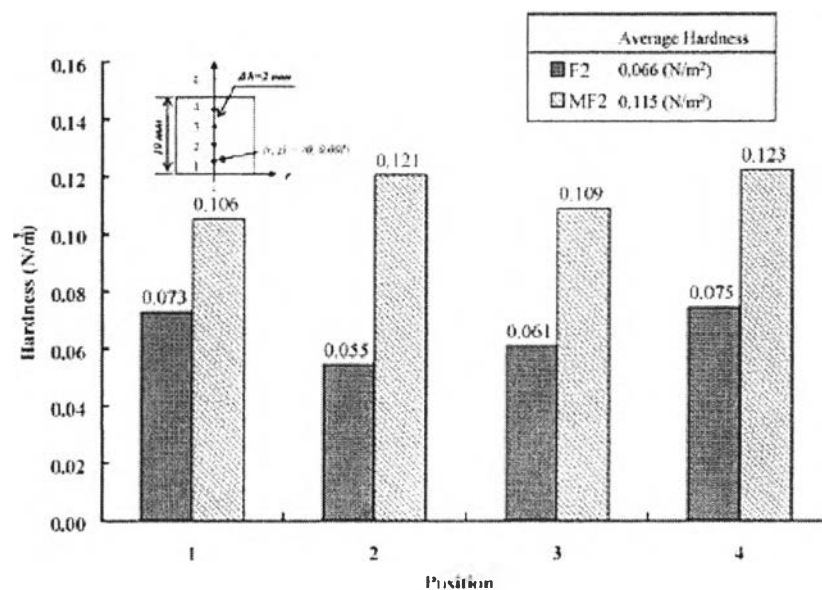


**Figure 2.15** Hardness results for samples prepared via slow freezing rate: F2 = chitosan/xanthan gum and MF2 = chitosan/xanthan gum/Na-MMT (Lui *et al.*, 2011).

The SEM micrograph showed the well interconnect pores occurred in all samples. The addition of Na-MMT slightly increased the pore size; however the pore size was surely depended on the freezing front velocity.

Pojanavaraphan *et al.* (2010) developed the form liked materials based on casein and Na-MMT clay using DL-glyceraldehyde (GC) as a crosslinking agent. The foam liked structure was produced by freeze-drying process. The Na-MMT aqueous suspension was slowly added in to casein-GC solution with the GC to casein ratio was 1:20. The mixture was frozen at  $-80^{\circ}\text{C}$  and freeze-dried in lyophilizer for 4 days and post cured at  $80^{\circ}\text{C}$  for 24 h. They suggested that GC was chosen because it was non-toxicity when compared with glutaraldehyde (GT), the common aldehyde used to crosslink protein. However, GC had low reactivity so it required post curing at high temperature. The incorporation of GC resulted in the higher compressive modulus and toughness. Adding of 5% (w/w) GC increased compressive modulus and toughness at 30% stain from 3900 to 5600 and 58 to 72 kPa, respectively. The addition of GC was also slightly increased the thermal stability. The higher casein content gave higher mechanical and thermal properties due to the continuous

architecture in the layers were connected by polymer. Moreover, the biodegradation study indicated that the casein and casein/Na-MMT aerogel exhibited low degradation rate compared with the degradation behavior of wheat starch since the house of card structure increased the time for degradation due to the microorganisms was more difficult to approach the internal region.

### 2.3 Tissue engineering

Tissue engineering is the applied method using the combination of cells, engineering and materials to create artificial construct for regeneration of new tissue. Normally, method that uses to repair tissues is isolated specific cells through a small biopsy from human and grows them on the three-dimensional scaffold under control conditions. The other alternative method is implanted scaffold for tissue ingrowth directly *in vivo* to stimulate and to direct tissue formation. This method spends shorter time to recovery for the patient (Rezwan *et al.*,2006).

There are several requirements of scaffold for tissue engineering because the human's body is really complex and sensitive. First of all, biocompatible both in bulk and degraded product are the major requirement. Second, mechanical properties of the scaffold must be sufficient to provide the correct stress environment for the new tissues and not collapse during usable. The scaffold should be porous materials in order to facilitate the transportation of calls and nutrient. It should exhibit the appropriate surface structure and chemistry for cell attachment. For bone tissue engineering, the typical porosity is 90% and the pore diameter is at least 100 $\mu$ m. (Rezwan *et al.*,2006, Yang *et al.*, 2001)

#### ❖ Materials

The first characteristic of materials should be concerned are biocompatibility and biodegradability which not leaches the toxic products. The potential materials with these characteristic include metal, polymer, and ceramic.

*Metal* is extensively used for surgical implantation for a period of time. Typical metals used in this application are stainless steels, cobalt based-alloy and titanium-based alloys. Nevertheless, the disadvantages of metals effect to tissue engineerin application are non-biodegradable and the limitation of processibility.

*Polymer* including natural polymers such as collagen, starch, chitin, chitosan and synthetic polymers such as PLA, PGA, PCL, and PHBV etc. Although, natural polymers are closely simulate the native cellular milieu but their mechanical properties is poor and some natural polymers requires a specific solvent. Many synthetic polymers have been developed to overcome these problems. Furthermore, synthetic polymers can be produced under controlled conditions and can be controlled the materials impurities.

*Ceramic* is seemed to be too stiffness and brittle so the combination of ceramic and polymer is the common way to achieve the suitable material for tissue engineering. Bioceramic such as hydroxyapatite, bioactive glass or clay minerals, etc., show biocompatibility and have been used in the application of bone defect repair or artificial bone matrix.

#### ❖ Structure and design

The scaffold for tissue engineering required porous structure. The regeneration of tissues is depends on the porosity and pore size of supporting 3-D structure. A large surface area and highly porous materials enhance the cell attachment and growth due to the accommodation for transport nutrients and waste products. The pore size and porosity of the scaffold for bone regeneration are investigated by some researchers as shown in Table 2.4. The interconnected macropore-structure is another factor for desirable scaffold. If the pores are not interconnected, the diffusion of waste or nutrient and cell migration will be inhibited.

**Table 2.4** Studies defining optimal pore size for bone regeneration (Yang *et al.*, 2001)

Reference	Scaffold pore size ( $\mu\text{m}$ )	Porosity	Mineralize tissue ingrowth/comments
Klawitter <i>et al.</i>	Type I: 2-6 $\mu\text{m}$	33.5%	No tissue ingrowth
	Type II: 15-40 $\mu\text{m}$	46.2%	No bone ingrowth, fibrous tissue ingrowth
	Type III: 30-100 $\mu\text{m}$ 80% pore < 100 $\mu\text{m}$	46.9%	50 $\mu\text{m}$ of bone ingrowth, osteoid and fibrous tissue ingrowth
	Type IV: 60-100 $\mu\text{m}$ 63% pores < 100 $\mu\text{m}$	46.9%	20 $\mu$ og bone ingrowth by 11 weeks and 500 $\mu\text{m}$ of ingrowth by 22 weeks, osteoid and fibrous tissue ingrowth
	Type V: 60-100 $\mu\text{m}$ 37% < 100 $\mu\text{m}$	48.0%	600 $\mu\text{m}$ of bone ingrowth by 11 weeks, osteoid and fibrous tissue ingrowth
Whang <i>et al.</i>	$\leq 100 \mu\text{m}$	35.3%	Not statistically different from untreated controls
	$\leq 200 \mu\text{m}$	51.0%	Not statistically different from untreated controls
	$\leq 350 \mu\text{m}$	73.9%	Statistically significant more bone than all other groups

A futher concern is the mecanical properties which should maintain the load for the required time without failure. To achieve the good strength, the scaffold must have the sufficiently interatomic and intermolecular bonding. (Hutmacher, 2000, Yang *et al.*, 2001, Rezwan *et al.*, 2006)